Semiconductors, 2023, Vol. 57, No. 4

Temperature Dependence of Dislocation-Related Electroluminescence in Silicon Light-Emitting Diodes Containing Oxygen Precipitates

© *N.A. Sobolev, A.E. Kalyadin, K.F. Shtel'makh, P.N. Aruev, V.V. Zabrodskiy, E.I. Shek*

Ioffe Institute,
194021 St. Petersburg, Russia

E-mail: nick@sobolev.ioffe.rssi.ru

Received April 7, 2023
Revised May 31, 2023
Accepted June 6, 2023

Electroluminescence has been studied in silicon light-emitting diodes containing oxygen precipitates at temperatures of 40−300 K. Oxygen ion implantation and multistage anneals are used for fabrication of the diodes. Over all temperature range, spectra are well approximated by one Lorentz and four Gaussian curves. Lines of dislocation-related luminescence D1−D4 (the D1 line is described by Lorentz curve) and oxygen precipitates (OPs) are present in the spectra. At temperature variation, peak positions of the D1, OP and D2 lines coincide with temperature dependence of the forbidden gap width reduced by values of 356, 330 and 303 meV respectively. Build and quenching areas are observed on temperature dependences of the electroluminescence intensities of the D1, OP and D2 lines, the activation energies of the processes are determined, and reasons of their appearance are discussed.

Keywords: Light-Emitting Diodes, Dislocation-Related Luminescence, Silicon, Oxygen Precipitates.

DOI: 10.61011/SC.2023.04.56427.4810

1. Introduction

Since the discovery of dislocation photoluminescence (PL) in silicon at liquid helium temperatures [1], there have been numerous studies of various process methods aimed at increasing the intensity of dislocation-related luminescence (DRL) and the temperature at which it is observed (see [2–4] and the literature therein). The methods based on laser recrystallization [5], uniaxial compression [6] and implantation of Si^+ or Er^+-ions followed by annealing in a chlorine-containing atmosphere (CCA) [3,7] have proved to be the most successful, which allowed the development of light-emitting diodes (LEDs) with dislocation-related electroluminescence (EL) at room temperature. This has been achieved to a significant extent through the development of gettering techniques (phosphorus [5], aluminum [6], chlorine-containing atmosphere annealing [3,7]) and hydrogen passivation [6] of non-radiative recombination centers. In the technology of large integrated circuits, the so-called internal gettering method is widely used to create a high-quality thin near-surface layer in silicon (see [8] and the literature therein) in which device structures were formed. The essence of the method was that multistage annealings in the 650−1000°C temperature range were carried out, during which oxygen precipitates were formed in the depth of the wafer grown by the Czochralski method, serving as effective getters for rapidly diffusing impurities that are effective recombination centers. However, it turned out that oxygen precipitates under certain conditions create dislocations which, on the one hand, can be effective centers of non-radiative recombination, and on the other — contribute to the creation of DRL centers. A number of papers [9,10] have been devoted to the study of the luminescent properties of these centers. Even structures with a PL maximum in the area ~ 1600 nm at room temperature [10] have been fabricated, but there was no information on the fabrication of oxide precipitate-containing LEDs with DRL in the literature. Recently, we have shown that additional oxygen ion implantation combined with multistage annealing allows to increase the DRL intensity and fabricate a LED operating at room temperature [11,12]. The aim of the present paper was to investigate the luminescent properties of LEDs containing oxide precipitates over a wide temperature range.

2. Experiment procedure

A wafer of *n*-type conductivity silicon of KEF-4.5 (100) grade grown by the Czochralski method was used to fabricate the LEDs. The oxygen and carbon contents measured by the IR absorption method are equal $\sim 8 \cdot 10^{17}$ and less than $2 \cdot 10^{16}\,\mathrm{cm}^{-3}$ respectively. To create a homogeneous distribution of oxygen atoms at a depth of 0.3–0.8 μm with a concentration of $5 \cdot 10^{19}\,\mathrm{cm}^{-3}$, implantation of the ions O^+ was carried out at room temperature. The implantation conditions were calculated using the SRIM-2013 [13,14] program. The ion energies were 350, 225, and 150 keV, and the corresponding ion doses were $1.5 \cdot 10^{15}$, $0.9 \cdot 10^{15}$, and $0.7 \cdot 10^{15}\,\mathrm{cm}^{-2}$. To dissolve oxygen growth precipitates, anneal radiation defects, form oxygen precipitates, dislocations, and other extended defects, three-stage annealings in argon flow at temperatures and times 1000°C/15 min + 650°C/7 h + 800°C/4 h were carried out. A final annealing at 1000°C for 6 h in a chlorine-containing atmosphere, which is an oxygen stream

saturated with carbon tetrachloride vapor with a molar concentration of 1%, was used to create DRL centers and gettering rapidly diffusing impurities. The LEDs were manufactured using planar technology. To create an $p^+{-}n$ transition on the implantation side of the ions O^+, windows with a diameter of 2 mm in the SiO_2 layer were opened, and a highly boron-doped p^+-layer of polycrystalline silicon (poly-Si) was deposited by gas-phase deposition. To create an ohmic contact, a heavily phosphorus-doped n^+-layer poly-Si was deposited on the backside of the wafer. The layers were deposited at 850° for 6 min, the concentration of doping impurities was $\sim 10^{20}\,\text{cm}^{-3}$, and the thickness of the layers was $\sim 0.5\,\mu$m. The contacts were formed by sputtering $0.5\,\mu$m thick aluminum. EL spectra in the 1000−1650 nm range were measured using an automated spectrometer based on an MDR-23 monochromator and an uncooled InGaAs photodiode. EL measurements were performed over a temperature range of 40−300 K with a temperature maintenance accuracy $\pm 1°$C. EL was excited by rectangular direct current pulses with a duration of 15 ms, an amplitude up to 25 mA, and a frequency of 32 Hz. The unit resolution was 5 nm.

3. Experimental results and discussion

Fig. 1 shows the EL spectra at temperatures of 40−300 K. The current density was 0.86 A/cm^2. The spectra are dominated by the DRL D1 line. With growth of the measurement temperature, there is first a short-wave and then a long-wave shift of its maximum and a non-monotonic change in its intensity. Second in intensity is the D2 line, whose maximum position at 40−80 K is at ∼ 1400 nm. The less intense D3 (∼ 1350 nm) and D4 (∼ 1240 nm) DRL lines are also present in the spectra. The absence of a relatively sharp decline between D1 and D2 lines in the temperature area 40−110 K is noteworthy, which may be due to the presence of an additional center.

EL spectra are a set of individual lines that overlap with each other. Traditionally, the spectra are decomposed into several constituent peaks using Gaussian curves at a fixed temperature [9,15] to identify individual lines. An example of the spectrum decomposition at 40 K is shown in Fig. 2. The wavelength values at the maxima of the curves 1521, 1471, 1406, 1337 and 1261 nm indicate that they belong to the luminescent centers D1, OP, D2, D3 and D4, respectively [2,3,6,9,11,16–19]. The unusual feature of this case of least-squares modelling is that the minimum deviation of the calculated curve from the experimental curve is achieved when the most intense line (D1) is represented by a Lorentz curve, and the other lines — when Gaussian curves are used. The occurrence of such a feature seems to be due to the qualitative difference (reconstruction) of the defective structure of the center D1 formed with the participation of oxygen precipitates compared to other technological methods. It is interesting to note that the OP line is not observed directly in this paper as a peak in the EL spectra, but is clearly visible in the decomposition of the EL spectrum. Incidentally, it was suggested to belong to oxygen precipitates in [17] after decomposition of the PL spectrum of a plastically deformed sample grown by the Czochralski method and doped with nitrogen; but it was also not observed as a separate peak. In [20] it was proven to belong to free oxygen precipitates. Recently in the paper [11], the OP line was clearly observed as a separate peak in the PL spectra of structures that have undergone the same, as in the studied LED, four-stage annealing, and within the error of experiments, its position in the spectrum coincided with the above wavelength value.

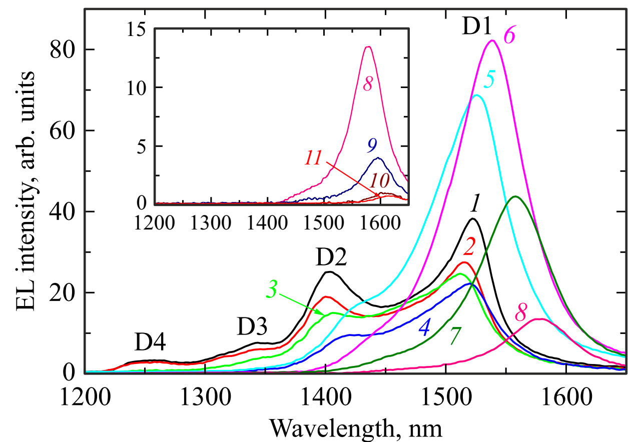

Figure 1. EL spectra of LED at different temperatures T, K: *1* — 40, *2* — 50, *3* — 80, *4* — 110, *5* — 140, *6* — 170, *7* — 200, *8* — 230, *9* — 260, *10* — 290, *11* — 300.

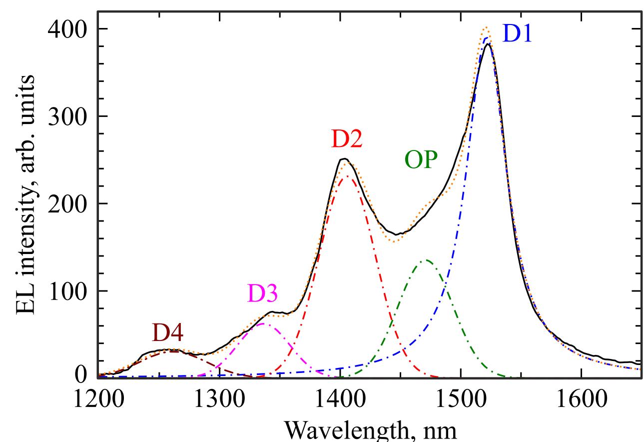

Figure 2. Decomposition of the EL spectrum measured at 40 K. Solid line — experimental curve. Dash and dot lines — components whose maxima are indicated in the text. The dot line — the total approximating curve.

Fig. 3 shows the values of positions of maxima of lines D1, OP and D2 as a function of temperature. For all three lines at temperatures > 50−70 K, a shift of the EL line to the long-wavelength side is observed. The approximation of dependences (solid lines) for D1 and D2

lines has shown that their positions $E(T)$ change parallel to the silicon band gap width $Eg(T)$ reduced by some constant value ΔE, which does not depend on temperature, and is described by the formula

$$E(T) = Eg(T) - \Delta E, \quad (1)$$

where $Eg(T) = 1169-0.49\,T^2/(T+655)$ [21], energy is measured in meV, and temperature T — in degrees Kelvin. In studied LED with oxygen precipitates for D1 line $\Delta E = 356$ meV, the well matches with the corresponding values for LED produced by uniaxial compression 362 meV [6] and light-emitting structures formed by electron irradiation 358 meV [18]. For D2 line $\Delta E = 303$ meV, which is almost identical to the value of 299 meV from [6]. Another characteristic feature of the temperature dependences of the positions of D1 and D2 lines is an anomalous shift to the short-wave side in the initial area from 40 to 70 K. Similar behavior for these lines was observed in [6,22] and explained by ionization of the doping impurity phosphorus. In this case, the excess of the maximum value of the energy position of the D1 and D2 lines over the approximating curves in our structures (for D1 line at 70–100 K $\sim$ 12 meV, and for D2 line at 50–60 K 20 meV) and structures obtained by uniaxial compression (for D1 line at 50–60 K $\sim$ 20 meV, and for D2 line at 60 K $\sim$ 15 meV) differ slightly.

For the OP line, the temperature dependence of the position of its maximum was measured for the first time (Fig. 3, curve OP). As the temperature rises to 60 K, the peak of the line moves to the short-wave side and then — to the long-wave side. The behavior of the line is well approximated by the formula (1), where $\Delta E = 330$ meV. The excess of the maximum value of the energy position of the OP line over the approximating curve at 60–80 K does not exceed 12 meV. The data obtained indicate that the behavior of the position of lines belonging to extended defects (D1, D2 and OP) at temperature changes obeys

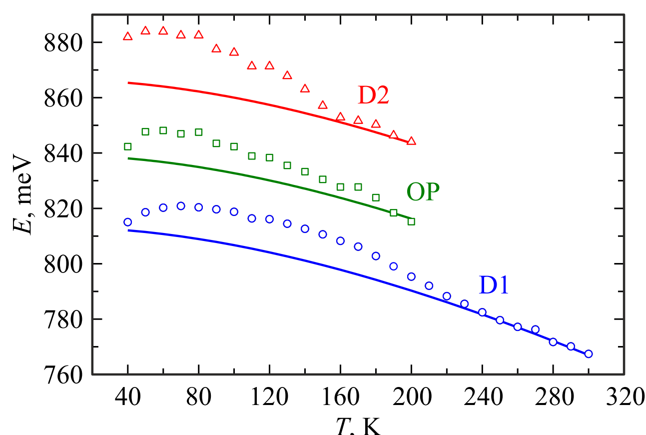

Figure 3. Temperature dependences of the energy positions of the maxima of the EL lines of D1, OD and D2 centers. Solid lines — approximation by the formula (1).

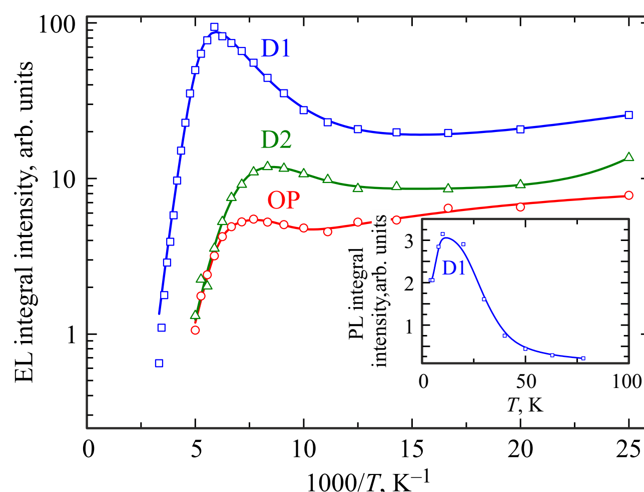

Figure 4. Dependences of integral intensities of EL lines D1, OP and D2 on the inverse temperature. Solid lines — approximation by formula (2). The insert shows the temperature dependence of the PL intensity for the D1 line from paper [11] (Fig. 2).

a general regularity. Note that a similar behavior of the peak maximum position from temperature was observed for another extended defect, the so-called {113} defect [23].

The dependence of the integral intensity of the EL D1 line on the inverse temperature is shown in Fig. 4. With growth in temperature, areas of quenching, buildup, and second quenching of the EL intensity are observed. This dependence is well approximated by the formula [24]

$$EL(T) = G/[1 + FT^{3/2}\exp(-K/kT)] + H/(\{1 + C/[1 + BT^{3/2}\exp(-E/kT)]\} \times [1 + DT^{3/2}\exp(-W/kT)]), \quad (2)$$

where K — the activation energy of EL quenching of center D1 at low temperature, E and W — the activation energies of buildup and EL quenching of center D1 at higher temperature respectively, C — a value including the ratio of charge carrier trapping cross sections on center D1 and traps, G, F, H, B and D — model parameters, k — Boltzmann constant.

The quenching of the EL intensity at low temperature (the first term in the formula (2)) is characterized by the quenching energy $K_{\mathrm{D1}} = 14.0$ meV and is related to the presence of the luminescent peak, which exists at $T < 40$ K. This is supported by the result of our previous paper [11] (Fig. 2), where it was found, that in a light-emitting structure, which is a wafer of silicon grown by the Czochralski method with high oxygen concentration ($\sim 8 \cdot 10^{17}$ cm^{-3}), subjected to multistage annealing under the same conditions as the investigated LED, with increasing measurement temperature the intensity of the PL line D1 increased and reached a maximum at 10–20 K, while in the range of 20–60 K it decreased by an order of magnitude (see insert in Fig. 4). Interestingly, the presence of a PL

peak for the D1 center in the same temperature area was previously observed in samples obtained by direct bonding of silicon [25] wafers and implantation of ions Si^+ [26]. The rise in PL intensity with increasing temperature was explained by the fact that at low temperatures, excitons are trapped on small centers, and with increasing temperature they are released, diffuse, and then there is their trapping and subsequent radiative recombination on the luminescent center D1 [24]. The luminescence ignition energies in these studies differed (4 [25] and 6.8 meV [11]), which can be explained by the different energy positions of the small trapping centers depending on the sample fabrication technology [24]. The PL quenching energies were 11 [25], 12 [26], and 11.6 meV [11], which is close to the exciton thermal dissociation energy [27]. In the investigated sample, the quenching of the EL intensity is characterized by practically the same value of $K_{D1} = 12.0$ meV as the PL quenching energy in the sample from [11], and is due to the dislocation of excitons and the subsequent capture of charge carriers at deeper capture centers.

With further temperature increase, the intensity of the D1 line reaches a maximum at $T \sim 170$ K. The energies of buildup and quenching are $E_{D1} = 35$ and $W_{D1} = 197$ meV. The appearance of a second higher temperature PL peak of center D1 was previously observed in samples obtained by co-implantation of Si^+ and B^+ ions [26]. The authors proposed a model for the appearance of this maximum: the increase in the PL intensity is associated with the thermal release of charge carriers from deeper capture centers (levels), their capture at the D1 center and subsequent radiative recombination, and the quenching of the intensity — with a more efficient capture of the released charge carriers at the centers of non-radiative recombination than at the D1 center. The authors attributed the changes in the values of the maximum temperature and its intensity to changes in the spectrum of deep capture centers, the formation of which is caused by the modes of boron implantation. The same model explains the appearance of the second maximum in our sample. However, the spectrum of deep capture centers is determined by the conditions of oxygen ion implantation and subsequent annealing.

The dependences of the integral intensity D2 and OP of the EL lines on the inverse temperature are shown in Fig. 4 (curves D2 and OP). With temperature rise, as in the case of D1 center, areas of quenching, buildup and second quenching of the EL intensity are observed. These dependencies are also well approximated by the formula (2) [24]. By analogy with center D1, it is natural to relate the quenching of the EL intensity of centers D2 and OP at low temperatures to the presence of luminescent peaks existing at $T < 40$ K. However, the quenching energies of the low-temperature peaks for these centers $K_{OP} = 4.6$ and $K_{D2} = 32$ meV differ from the value for the D1 center. In [26] paper, it was found that additional implantation of B^+ ions is accompanied by a significant change in the quenching rate of the low-temperature PL peak of the D1 line at temperatures > 40 K, compared to the sample implanted with Si^+ ions alone. The authors attributed this effect to changes in the structure D1 center and the energy spectrum of the sample. It is reasonable to assume that the change in the quenching energy of the low-temperature EL peak of the D2 and OP centers is due to the difference in the structure of these luminescent centers. With increasing temperature, the intensity dependences of EL D2 and OP centers also had maxima at ~ 120 and 130 K respectively. The buildup and quenching energies of the EL intensity are $E_{D2} = 67$, $E_{OP} = 117$, $W_{D2} = 104$ and $W_{OP} = 178$ meV. The appearance of these high-temperature maxima is explained using the same model that was proposed for samples obtained by co-implantation of Si^+ and B^+ ions [26]. The differences in the buildup and quenching energies of the EL intensity are due to the fact that different deep levels are involved in carrier capture and subsequent radiative and non-radiative recombination for the D2 and OP centers.

4. Conclusion

The effect of measurement temperature in the range of 40−300 K on the luminescence properties of silicon LEDs fabricated by implantation of ions O^+ and four-step annealing at 650−1000°C temperatures, in which D1 DRL line is recorded at room temperature, has been investigated. A set of overlapping lines is observed in the spectra of the EL. A multi-component decomposition of the spectra was performed to identify the parameters of the individual lines, which revealed the formation of four D1−D4 DRL lines and an OP line belonging to free oxygen precipitates. Thus D1 line is described by a Lorentz curve, and the other — Gauss curves. With changing temperature, the positions of the peaks of the D1, OP, and D2 lines move parallel to the silicon band gap width, reduced by values of 356, 330, and 303 meV respectively. The behavior of the peaks D1 and D2 lines correspond well with data obtained on samples fabricated using other techniques. The temperature dependence of the position of the OP line in the EL spectrum was obtained for the first time. The temperature dependences of the intensities of D1, OP and D2 lines are not monotonic, but their behavior is uniform. As the temperature increases, a decrease in intensity is observed, which is a continuation of the decline in intensity of the low-temperature peak whose maximum is below 40 K. As the temperature increases further, a high-temperature peak is formed. Its intensity rise is due to the release of charge carriers trapped on deep traps, their trapping on the luminescent center and subsequent radiative recombination. The quenching of the high-temperature peak is associated with the trapping of charge carriers at deeper centers of nonradiative recombination. The activation energies of quenching and buildup of the EL intensities for all three lines were determined. The differences in the buildup and quenching energies of the EL intensity are due to the fact that different deep levels are involved in the

capture of charge carriers and subsequent radiative and non-radiative recombination for centers D1, OP and D2. The appearance of high-temperature luminescence peaks D1 line in samples containing oxide precipitates and D2 line in samples fabricated by different methods was observed for the first time. The temperature dependence of the electroluminescence intensity of the OP and D2 center has not been previously investigated.

Conflict of interest

The authors declare that they have no conflict of interest.

References

[1] N.A. Drozdov, A.A. Patrin, V.D. Tkachev. JETP Lett., **23**, 597 (1976).
[2] N.A. Sobolev. Semiconductors, **44** (1), 1 (2010).
[3] N.A. Sobolev, A.E. Kalyadin, M.V. Konovalov, P.N. Aruyev, V.V. Zabrodsky, E.I. Shek, K.F. Shtelmakh, A.N. Mikhailov, D.I. Tetelbaum. Semiconductors, **50** (2), 240 (2016).
[4] A. Tereshchenko, D. Korolev, M. Khorosheva, A. Mikhaylov, A. Belov, A. Nikolskaya, D. Tetelbaum. Phys. Status Solidi A, **216**, 1900323 (2019).
[5] E.O. Sveinbjornsson, J. Weber. Appl. Phys. Lett., **69**, 2686 (1996).
[6] V. Kveder, V. Badylevich, E. Steinman, A. Izotov, M. Zeibt, W. Schreter. Appl. Phys. Lett., **84**, 2106 (2004).
[7] N.A. Sobolev, A.M. Emel'yanov, V.V. Zabrodskii, N.V. Zabrodskaya, V.L. Sukhanov, E.I. Shek. Semiconductors, **41** (5), 616 (2007).
[8] A. Borghesi, B. Pivac, A. Sassella, A. Stella. J. Appl. Phys., **77**, 4169 (1995).
[9] S. Binetti, S. Pizzini, E. Leoni, R. Somaschini, A. Castaldini, A. Cavallini. J. Appl. Phys., **92**, 2437 (2002).
[10] K. Bothe, R.J. Falster, J.D. Murphy. Appl. Phys. Lett., **101**, 032107 (2012).
[11] N.A. Sobolev, A.E. Kalyadin, K.F. Shtel'makh, E.I. Shek. Semiconductors, **55** (12), 891 (2021).
[12] N.A. Sobolev, A.E. Kalyadin, K.F. Shtel'makh, P.N. Aruev, V.V. Zabrodskiy, E.I. Shek. Semiconductors, **56** (9), 685 (2022).
[13] J.F. Ziegler, M.D. Ziegler, J.P. Biersack. Nucl. Instr. Meth. B, **268**, 1818 (2010).
[14] http://www.srim.org
[15] N.A. Sobolev, A.M. Emel'yanov, E.I. Shek, O.V. Feklisova, E.B. Yakimov, T.V. Kotereva. Phys. Status Solidi C, **2** (6), 1842 (2005).
[16] R. Sauer, J. Weber, J. Stolz, E.R. Weber, K.H. Kurster, H. Alexander. Appl. Phys. A, **36**, 1 (1985).
[17] S. Binetti, R. Somaschini, A. Le Donne, E. Leoni, S. Pizzini, D. Li, D. Yang. J. Phys.: Condens. Matter, **14**, 13247 (2002).
[18] Luelue Xiang, Dongsheng Li, Lu Jin, Shuming Wang, Deren Yang. J. Appl. Phys., **113**, 033518 (2013).
[19] L.I. Fedina, A.K. Gutakovskii, T.S. Shamirzaev. J. Appl. Phys., **124**, 053106 (2018).
[20] V.I. Vdovin, L.I. Fedina, A.K. Gutakovskii, A.E. Kalyadin, E.I. Shek, K.F. Shtel'makh, N.A. Sobolev. Crystallogr. Rep., **66**, 625 (2021).
[21] V. Alex, S. Finkbeiner, J. Weber. J. Appl. Phys., **79**, 6943 (1996).
[22] E.A. Steinman, A.N. Tereshchenko, N.V. Abrosimov. Solid State Phenomena, **131**–**133**, 607 (2008).
[23] A.E. Kalyadin, K.F. Shtelmakh, P.N. Aruev, V.V. Zabrodsky, K.V. Karabeshkin, E.I. Shek, N.A. Sobolev. Semiconductors, **54** (6), 687 (2020).
[24] G. Davies. Phys. Reports, **176**, 83 (1989).
[25] E.A. Steinman, O. Kononchuk, A.N. Tereshchenko, A.A. Mazilkin. Solid State Phenomena, **156**–**158**, 555 (2010).
[26] A.N. Tereshchenko, D.S. Korolev, A.N. Mikhailov, A.I. Belov, A.A. Nikolskaya, D.A. Pavlov, D.I. Tetelbaum, E.A. Steinman. Semiconductors, **52** (7), 843 (2018).
[27] K.L. Shaklee, R.E. Nahory. Phys. Rev. Lett., **24**, 942 (1970).

Translated by Y.Deineka